# Novel Microstrip Coupled-Line Bandpass Filters With Shortened Coupled Sections for Stopband Extension

Chao-Huang Wu, Yo-Shen Lin, Chi-Hsueh Wang, and Chun Hsiung Chen, *Fellow, IEEE*

***Abstract*—Novel microstrip coupled-line bandpass filters with extended rejection band are proposed using the transmission zeros inherently associated with the shortened coupled sections to suppress the odd spurious harmonics at $(2n+1)f_o$ $(n=1,2,\ldots)$, where $f_o$ is the passband center frequency. The proposed filters feature compact size and low insertion loss, and have two cross-coupled-induced transmission zeros near the passband edges for improving the filter selectivity. To demonstrate this novel technique of shortening coupled sections, the second-order filter with the stopband extended up to $4.6f_o$ is implemented and carefully examined. To further improve the filter response, the fourth-order filter with the rejection extended up to $7.4f_o$ and better than 30 dB is also implemented.**

***Index Terms*—Bandpass filter, coupled line, microstrip, stopband extension.**

## I. Introduction

BANDPASS filters with the characteristics of low insertion loss, compact size, high selectivity, and good stopband rejection are highly required in next-generation mobile and satellite communication systems. Among various types of planar filters, one of the most common implementations is based on the parallel-coupled transmission-line structures. Following simple synthesis procedure, the required coupled-line parameters can easily be derived from the given specifications. However, the conventional microstrip parallel-coupled filters suffer from the drawback of out-of-band spurious responses at $nf_o(n=2,3,\ldots)$ due to the unequal even- and odd-mode propagation constants associated with the microstrip coupled-line sections [1], [2].

To reject the second harmonic response at $2f_o$, several techniques have been reported [3]–[12]. A capacitive compensation of phase velocity difference in parallel-coupled microstrip line was employed in suppressing the spurious response at $2f_o$ [3]. In [4], the over-coupled resonators were proposed to extend the electrical length of the odd mode so as to compensate for the difference in the phase velocities. The acute sawtooth coupled lines were adopted to equalize the electrical lengths of the $c$- and $\pi$-mode in [5]. The wiggly-line filters using a sinusoidally varying linewidth were proposed to give an effective suppression on the second harmonic response [6]. A proper height of substrate suspension [7], [8] and ground-plane aperture [9] were also used to equalize the even- and odd-mode phase velocities so that the second harmonic response can be rejected. In [10], the split-ring resonators (SRRs) were introduced to obtain strong magnetic coupling for spurious passband suppression. In [11], the image impedance of coupled-line sections was increased to reduce the difference between even- and odd-mode phase constants. Recently, a meandered parallel coupled line was adopted to speed up the even-mode phase velocity such that the spurious passband at $2f_o$ can be suppressed [12]. In [13], the step-impedance resonator (SIR) with a large impedance ratio and adjustable higher order transmission zeros were utilized to increase the rejection bandwidth. However, most of these filter structures still suffer from third and higher harmonic spurious responses [3]–[12], and the design procedure of the filters in [13] is quite complex.

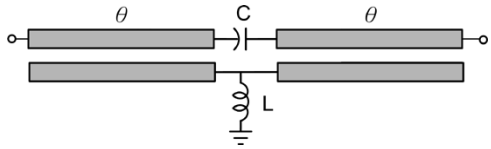


Fig. 1. Circuit model of second-order coupled-line filter in [14]–[16].

In our previous papers, [14]–[16], novel compact coupled-line filters were proposed by using additional lumped-elements to realize $K$-inverters in conventional parallel-coupled bandpass filter structures. With the introduction of the cross-coupled effect, two transmission zeros at upper and lower stopbands can be designed at the desired locations for improved filter selectivity. In addition, due to the equivalence to the quarter-wavelength $(\lambda/4)$ resonator filter, these filters occupy only half the circuit area of conventional ones and feature no spurious responses at even harmonics in nature. The corresponding second-order filter circuit model in [14]–[16] is shown in Fig. 1.

In this paper, the concept in [14]–[16] is extended by adopting the inherent transmission zeros associated with the shortened coupled sections to suppress the spurious harmonics so that a coupled-line filter with very wide rejection band may be achieved. Specifically, all the second, third, fourth, fifth and sixth harmonics may be suppressed. The advantage of

Manuscript received January 18, 2005; revised August 31, 2005. This work was supported by the National Science Council of Taiwan under Grant NSC 93-2752-E-002-001- PAE and Grant NSC 93-2219-E-002-021.

C.-H. Wu, C.-H. Wang, and C. H. Chen are with the Department of Electrical Engineering and the Graduate Institute of Communication Engineering, National Taiwan University, Taipei 106, Taiwan, R.O.C. (e-mail: chchen@ew.ee.ntu.edu.tw).

Y.-S. Lin was with the Graduate Institute of Communication Engineering, National Taiwan University, Taipei 106, Taiwan, R.O.C. He is now with the Department of Electrical Engineering, National Central University, Chungli 320, Taiwan, R.O.C.

Digital Object Identifier 10.1109/TMTT.2005.862710

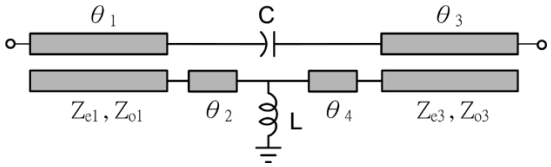


Fig. 2. Circuit model of proposed second-order coupled-line filter with shortened coupled sections for extension of rejection band.

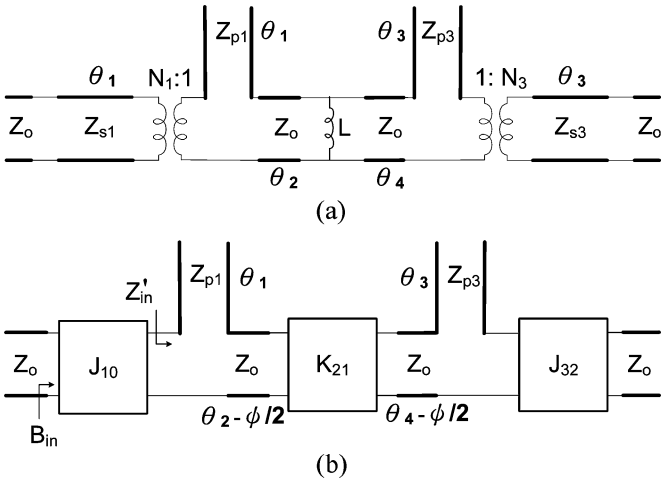


Fig. 3. Equivalent-circuit models for the proposed second-order coupled-line filter in Fig. 2 without the cross-coupling effect. ($N_n = (Z_{oen} + Z_{oon})/(Z_{oen} - Z_{oon})$, $Z_{sn} = (Z_{oen} + Z_{oon})/2$, $Z_{pn} = 2Z_{oen}Z_{oon}/(Z_{oen} + Z_{oon})$, $J_{n,n-1} = |2/(Z_{oen} - Z_{oon})|$, $n = 1, 3, K_{21} = Z_o \tan|\psi/2|$.)

the proposed structure is that it provides effective stopband extension with a very compact circuit size.

## II. Second-Order Filter

### A. Filter Structure

Shown in Fig. 2 is the circuit model of the proposed second-order coupled-line filter for stopband extension. Here, the lumped-element inductor $L$ is included to realize a $K$-inverter, and the cross-coupled capacitor $C$ is introduced to achieve two transmission zeros, as in [14]–[16], so that the filter performance may be improved. Compared with Fig. 1, the lengths $(\theta_1, \theta_3)$ of the coupled sections are shortened with two additional transmission-line sections $(\theta_2, \theta_4)$ included to maintain the $\lambda/4$ resonators in constructing the filter.

By neglecting the series cross-coupled capacitor, i.e., $C = 0$, and also based on the assumption that the even- and odd-mode phase velocities are equal, the equivalent-circuit model of the filter structure in Fig. 2 for the frequencies around the passband may first be represented by the one in Fig. 3(a) [17, Sec. 5.09]. Specifically, the input open-ended coupled-line section of length $\theta_1$ in Fig. 2 may be modeled by an ideal transformer of turn ratio $N_1 = (Z_{oe1} + Z_{oo1})/(Z_{oe1} - Z_{oo1})$ with a transmission line of characteristic impedance $Z_{s1} = (Z_{oe1} + Z_{oo1})/2$ and a series open stub of characteristic impedance $Z_{p1} = 2Z_{oe1}Z_{oo1}/(Z_{oe1} + Z_{oo1})$ at its two ends, as shown in Fig. 3(a) [17, Sec. 5.09]. Similar modeling may also be applied to the output open-ended coupled-line section of length $\theta_3$.

Since the value of $Z_{sn}(n = 1, 3)$ and that of the reference impedance $Z_o$ are nearly the same, the transmission line of characteristic impedance $Z_{sn}$ and length $\theta_n$ together with additional transmission line of characteristic impedance $Z_o$ may be combined with the ideal transformer to form the $J$-inverter $(J_{n,n-1})$, as shown in Fig. 3(b) [18, Sec. 8.7], where $J_{n,n-1} = |2/(Z_{oen} - Z_{oon})|(n = 1, 3)$. Besides, the shunt inductor $L$ with two transmission-line sections of characteristic impedance $Z_o$ and length $\psi/2$ at its two sides may be equivalent to a $K$-inverter $(K_{21} = Z_o \tan|\psi/2|)$, as shown in Fig. 3(b) [17, Sec. 8.03]. Thus, by combining the above processes, one may finally yield the equivalent-circuit model, as shown in Fig. 3(b).

Note that the inverters in Fig. 3(b) satisfy the conditions $K_{21}/Z_o \ll 1$ and $J_{n,n-1}/Y_o \ll 1(n = 1, 3)$ [19]. Thus, near the center frequency and by letting the input susceptance $B_{\text{in}}$ in Fig. 3(b) equal to the susceptance $B_1$ given in the bandpass prototype [19, Fig. 6], one may establish a relation for determining the coupled-line impedances ( $Z_{oe1}$, $Z_{oo1}$)

$$\begin{aligned} B_{\text{in}} &= \frac{4}{(Z_{oe1} - Z_{oo1})^2}\left[Z_o \tan\frac{\left(\theta_2 - \frac{\phi}{2}\right)\omega}{\omega_o} - Z_{p1}\cot\frac{\theta_1\omega}{\omega_o}\right] \\ &= \frac{g_1}{\Delta Z_o}\left(\frac{\omega}{\omega_o} - \frac{\omega_o}{\omega}\right) \\ &= B_1. \end{aligned} \tag{1}$$

Here, $Z_o$ is the reference impedance, $\omega_0$ is the radian center frequency, $\Delta$ is the 3-dB bandwidth, and $g_1$ is the element value of the low-pass filter prototype [17]. In order to maintain the $\lambda/4$ resonators at the center frequency $(\theta_1 + \theta_2 - \psi/2 = \pi/2)$, the input impedance $Z'_{\text{in}}$ in Fig. 3(b) should satisfy the resonance condition ($\text{Im}\{Z'_{\text{in}}\} = 0$ or $Z_o = Z_{p1}$), which implies

$$(Z_{oe1} + Z_{oo1})Z_o = 2Z_{oe1}Z_{oo1}. \tag{2}$$

When $\theta_1$ (or $\theta_3$) $= 180°$ at certain frequencies, the series open stubs in Fig. 3(b) are open circuited such that the transmission zeros may be created at those frequencies. Thus, the stub lengths $(\theta_1, \theta_3)$ can be designed to adjust the locations of the transmission zeros.

### B. Transmission Zeros

To examine the effect of the shortened coupled sections for the filter in Fig. 2, the simulated insertion loss responses of the microstrip coupled-line sections with different electrical lengths $\theta$ at $f_o = 2$ GHz are shown in Fig. 4. For the ideal case in which the even- and odd-mode electrical lengths are equal $(\theta_e = \theta_o)$, the $|S_{21}|$ response for the coupled-line section of $\theta = 90°$ at $f_o$ has an inherent transmission zero at $2f_o$, while that for the case of $\theta = 60°$ has an inherent transmission zero at $3f_o$. For the practical microstrip coupled line, the inherent transmission zero moves to higher frequencies due to the unequal even- and odd-mode phase constants [11]. As shown in Fig. 4, the microstrip coupled-line section of $\theta = 67°$ would have an inherent transmission zero at around $3f_o$. Therefore, by taking advantage of the inherent transmission zeros associated with the coupled-line sections, the coupled-line lengths $\theta_1$ and $\theta_3$ in

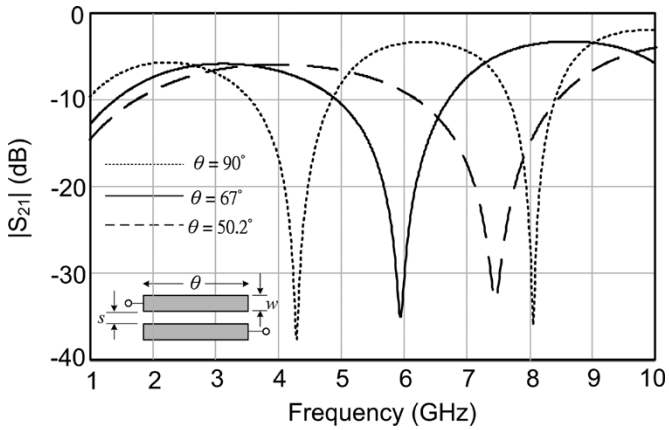


Fig. 4. Adjustment of the electrical length $\theta$ (at$f_o = 2$ GHz) of microstrip coupled-line section to vary the location of inherent transmission zero. ($w = 2.5$ mm, $s = 0.5$ mm, substrate dielectric constant $\varepsilon_r = 3.38$, thickness $= 1.32$ mm.)

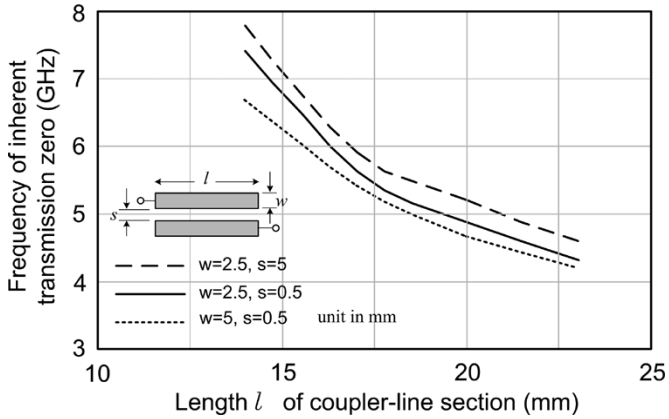


Fig. 5. Curves to relate the frequency of inherent transmission zero to the length $l$ of microstrip coupled-line section.

Fig. 2 may properly be chosen such that these inherent transmission zeros fall around $3f_o$ for suppression of the spurious passband. After $\theta_1$ and $\theta_3$ are fixed, two additional transmission lines should be added to compensate for the required electrical length of the $\lambda/4$ resonator filter in Fig. 2 such that $\theta_1 + \theta_2 = \theta_3 + \theta_4 = \pi/2 + \psi/2$.

The location of inherent transmission zero associated with the microstrip coupled-line section may properly be adjusted by its geometrical parameters, as illustrated in Fig. 5. Specifically, Fig. 5 shows the simulated curves to relate the frequency of inherent transmission zero to the length $l$ of the coupled-line section with its spacing $s$ and width $w$ as parameters. Among these three parameters, the length $l$ of the coupled-line section has much more influence on the inherent transmission-zero frequency, therefore, it would be the major parameter to control the location of the inherent transmission zero. In particular, the inherent transmission-zero frequency increases as the coupled-line length decreases, as described in Fig. 5, which will be used in the design of a filter for stopband extension.

The cross-coupled capacitor $C$ of the proposed filter structure in Fig. 2 is used to create a second cross-coupled path, along which the signal would cancel the one traveling along the main path at two frequencies such that two additional cross-coupled-induced transmission zeros may be created [14]–[16] for an improvement of filter selectivity. The locations of these cross-coupled-induced transmission zeros may be controlled by suitably adjusting the value of cross-coupled capacitance $C$. Fig. 6(a) shows the simulated responses of the filter circuit model in Fig. 2 for which the center frequency $f_o$ is designed at 2 GHz. Specifically, the two cross-coupled-induced transmission zeros will move toward the center frequency as the value of $C$ increases. Fig. 6(b) also shows the curves to relate the frequencies of cross-coupled-induced transmission zeros to the values of cross-coupled capacitance $C$. Based on these information, one may suitably choose the value of $C$ so that the locations of these cross-coupled-induced transmission zeros may be adjusted for the desired selectivity.

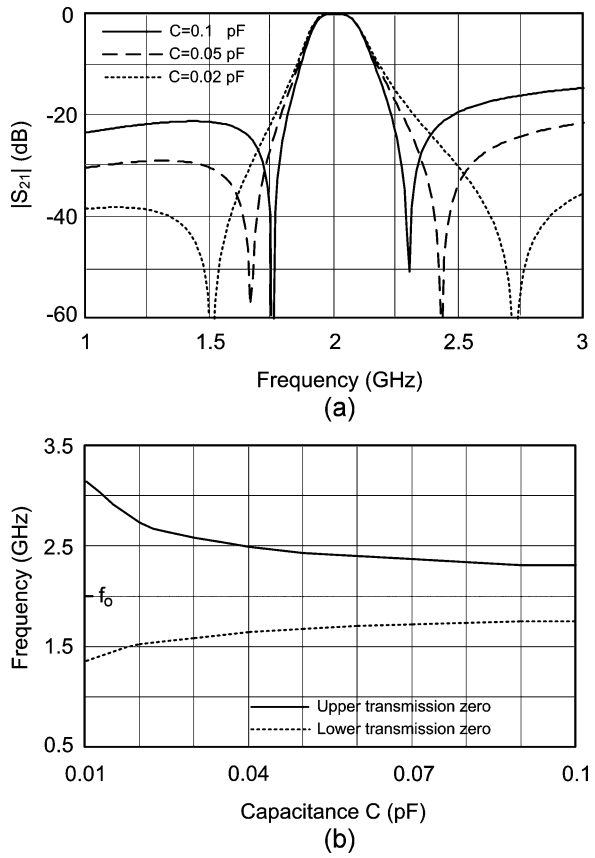


Fig. 6. (a) Simulated responses of the filter circuit model (Fig. 2) for various values of $C$. (b) Curves to relate the cross-coupled-induced transmission-zero frequencies to the values of $C$. ($\theta_1 = 51.8°$, $\theta_2 = 35°$, $\theta_3 = 61.8°$, $\theta_4 = 25°$, $L = 0.22$ nH, $Z_{oe1} = 69\ \Omega$, $Z_{oo1} = 39\ \Omega$, $Z_{oe3} = 66.3\ \Omega$, $Z_{oo3} = 39.8\ \Omega$.)

### C. Filter Implementation and Results

All proposed filter structures are implemented using the microstrip configuration, and are fabricated on the Rogers RO4003c substrate ($\varepsilon_r = 3.38$, $\tan\delta = 0.0023$, and thickness $h = 1.32$ mm).

The design procedures for the proposed second-order filter (Fig. 2) may be summarized as follows. First, according to the spurious harmonic frequencies to be suppressed, the required electrical lengths ($\theta_1$, $\theta_3$) are obtained.

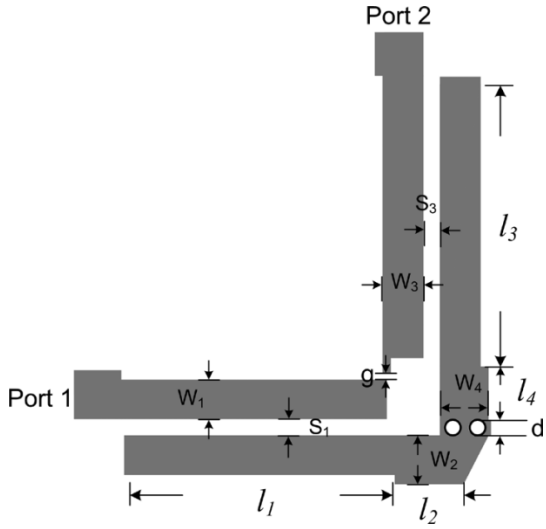


Fig. 7. Layout of the proposed second-order microstrip coupled-line bandpass filter with shortened coupled sections for stopband extension. ($W_1 = 2.5$ mm, $S_1 = 0.5$ mm, $l_1 = 17$ mm, $W_2 = 3.1$ mm, $l_2 = 4.4$ mm, $W_3 = 2.6$ mm, $S_3 = 0.55$ mm, $l_3 = 18$ mm, $W_4 = 3.1$ mm, $l_4 = 4.4$ mm, $d = 1$ mm, and $g = 0.4$ mm.)

Second, the coupled-line impedances $(Z_{oen}, Z_{oon})(n = 1, 3)$ are determined from (1) and (2) and the given filter specifications. Note that (1) is satisfied when $\omega$ is nearly equal to $\omega_0$, hence, the upper 3-dB radian frequency $\omega = (1 + \Delta/2)\omega_0$ is used in the computation.

Third, the required $K$-inverter value $(K_{21})$ in Fig. 3(b) is obtained based on the filter specifications through the conventional filter synthesis techniques, and from this $K_{21}$, the value of shunt inductance $L$ may then be determined [19].

Fourth, the value of cross-coupled capacitance $C$ is also determined by the desired locations of two transmission zeros. Finally, a fine-tuning based on an electromagnetic (EM) simulator such as HFSS is required to suitably suppress the spurious passband and maintain the main passband performance. A filter with wider stopband and a sharper falloff at the passband edges may then be achieved.

Shown in Fig. 7 is the layout of the proposed second-order microstrip coupled-line bandpass filter based on the circuit model in Fig. 2. The shunt inductor $L$ is implemented by a metal via to ground. The via-diameter is determined by the required $L$ value based on the closed-form expressions in [20]. The coupled-line sections are arranged like the modified parallel-coupled filter in [2] such that the cross-coupled capacitor $C$ can be realized by the gap-coupled capacitance between the open-ends of two coupled-line sections. In order to achieve the desired amount of cross-coupling, the two coupled-line sections are bent by an angle of 90 °. Note that the coupled-line sections should be suitably shortened so that their inherent transmission zeros are located around $3f_o$.

The filter is designed with a center frequency of 2 GHz, a 3-dB bandwidth of 9.3%, according to a second-order maximally flat response. The corresponding circuit parameters are obtained as follows: $Z_{oe1} = 65.8\,\Omega$, $Z_{oo1} = 40.5\,\Omega$, $Z_{oe3} = 65.3\,\Omega$, $Z_{oo3} = 40.7\,\Omega$, $\theta_1 = 70.2°$, $\theta_3 = 74.35°$ at 2 GHz, and $L = 0.22$ nH. The two coupled-line lengths $\theta_1$ and $\theta_3$ are made slightly different so as to improve and smooth the harmonic rejection. The geometrical parameters are then obtained by fine tuning in HFSS, and are given in Fig. 7.

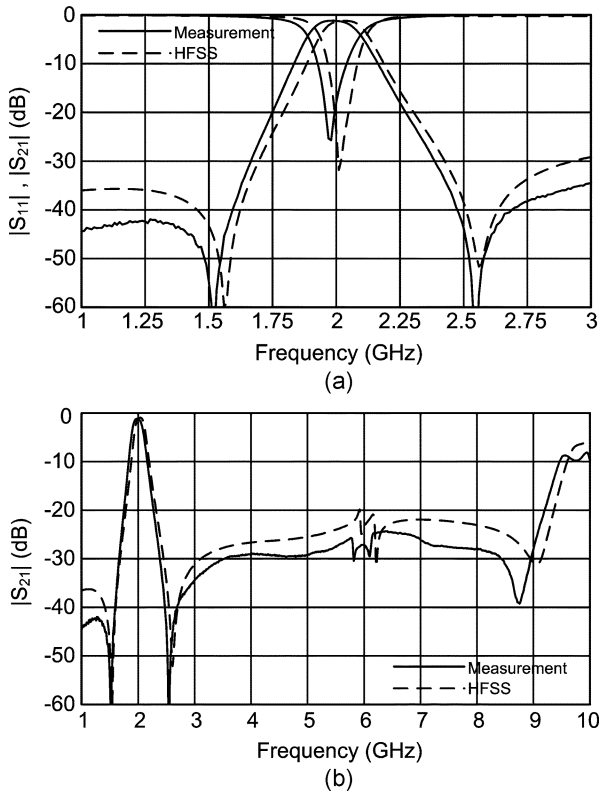


Fig. 8. Measured and simulated results for the proposed second-order microstrip bandpass filter in Fig. 7. (a) Narrow- and (b) wide-band frequency responses.


Fig. 9. Layout of the fourth-order microstrip coupled-line bandpass filter in [16].

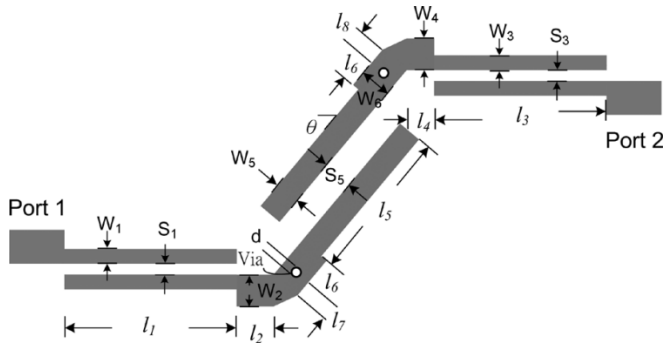


Fig. 10. Layout of the proposed fourth-order microstrip coupled-line bandpass filter with shortened coupled sections for stopband extension. ($W_1 = 1$ mm, $S_1 = 0.3$ mm, $l_1 = 16$ mm, $W_2 = 3.4$ mm, $l_2 = 4.4$ mm, $W_3 = 1$ mm, $S_3 = 0.4$ mm, $l_3 = 17$ mm, $W_4 = 3.4$ mm, $l_4 = 4.4$ mm, $W_5 = 3$ mm, $S_5 = 3$ mm, $l_5 = 19$ mm, $W_6 = 3.4$ mm, $l_6 = 0.5$ mm, $l_7 = 0.8$ mm, $l_8 = 1.35$ mm, $d = 0.7$ mm, and $\theta = 40°$.)

The measured and simulated results are shown in Fig. 8. The measured center frequency is at 1.98 GHz. The minimum measured insertion loss is 1.16 dB at 1.99 GHz, and the 3-dB band-

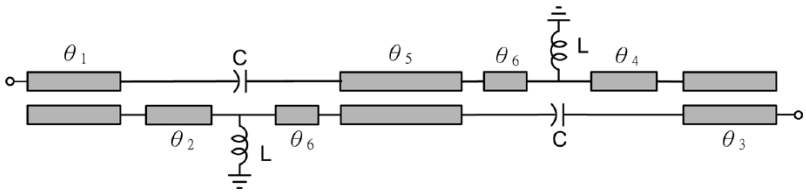


Fig. 11. Circuit model of the fourth-order coupled-line filter in Fig. 10.

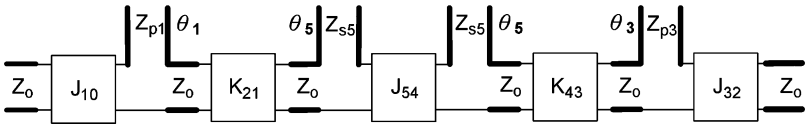


Fig. 12. Equivalent-circuit model for the proposed fourth-order coupled-line filter in Fig. 11 without the cross-coupling effect. Here, $(Z_{p1}, Z_{p3})$, $(J_{10}, J_{32})$, and $(K_{21}, K_{43})$ are defined inFig. 3, and $(Z_{s5}, J_{54})$ are defined inFig. 13.

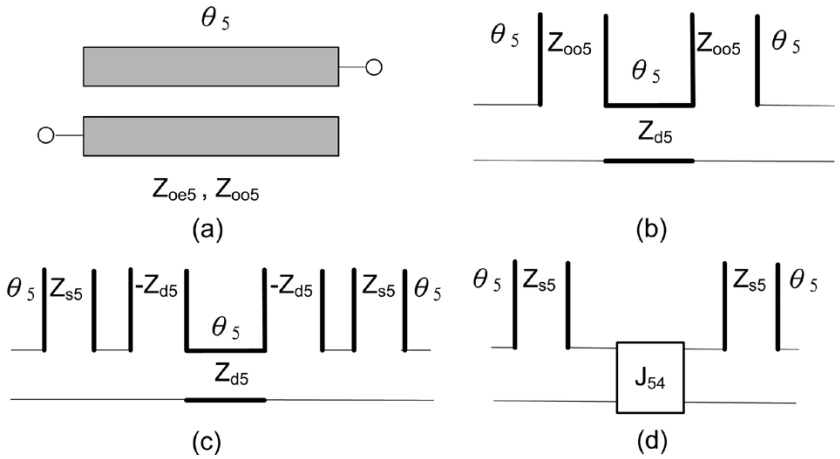


Fig. 13. Equivalence between: (a) coupled-line section and (d) the $J$-inverter with two series open stubs. ($Z_{d5} = (Z_{oe5} - Z_{oo5})/2$, $Z_{s5} = (Z_{oe5} + Z_{oo5})/2$, $J_{54} = |\sin\theta_5/Z_{d5}|$.)

width is 10%. The spurious responses are suppressed up to $4.6f_o$ due to the use of shortened coupled-line sections, and the harmonic rejection is better than 25 dB in the measured results. Two cross-coupled-induced transmission zeros are observed at 1.51 and 2.52 GHz, as expected. Good agreement between measured and simulated results is observed, except for a slight frequency shift.

## III. Fourth-Order Filter

To further improve the filter response, a novel fourth-order filter is implemented. For comparison, Fig. 9 shows the layout of the fourth-order microstrip filter discussed in [16] in which three coupled-line sections are used along with two shunt inductors to realize the $K$-inverters. Based on the principle of shortening the coupled-line sections, a novel fourth-order microstrip coupled-line bandpass filter with the layout shown in Fig. 10 is proposed so as to improve the stopband rejection. The corresponding circuit model is shown in Fig. 11. Two transmission zeros at the upper and lower stopbands would be created by the cross-coupled capacitors $C$ in Fig. 11. Similarly, the cross-coupled capacitor $C$ can be realized by the gap-coupled capacitance between the open-ends of coupled-line sections. In order to achieve the desired amount of cross-coupling, the coupled-line sections are bended by an angle of 40°. The lengths of the coupled-line sections are shortened again with additional transmission-line sections included so that the harmonics may be suppressed. The third harmonic response is suppressed by adjusting the lengths $l_1$ and $l_3$ of the coupled-line sections. Here, the lengths $l_1$ and $l_3$ are made slightly different so that the stopband rejection may be improved and smoothed. The fifth harmonic response is suppressed by the proper choice of the length $l_5$ of coupled-line sections.

By neglecting the series cross-coupled capacitors again, i.e., $C = 0$, the equivalent-circuit model for the proposed fourth-order coupled-line filter in Fig. 11 may be depicted in Fig. 12. As described in Section II-A, the input/output open-ended coupled-line sections of length $\theta_1$ and $\theta_3$ in Fig. 11 may be modeled by the $J$-inverters ( $J_{10}$ and $J_{32}$) along with the series open stubs of characteristic impedances $Z_{p1}$ and $Z_{p3}$. Besides, each shunt inductor $L$ with two transmission-line sections of characteristic impedance $Z_o$ and length $\psi/2$ at its two sides may be equivalent to a $K$-inverter ($K_{21}$ or $K_{43}$). The equivalence between the interstage coupled-line section of length $\theta_5$ in Fig. 11 and the $J$-inverter $(J_{54})$ in Fig. 12 may be demonstrated in Fig. 13.

The interstage open-ended coupled-line section of length $\theta_5$ in Fig. 13(a) may be modeled by a transmission-line section of characteristic impedance $Z_{d5} = (Z_{oe5} - Z_{oo5})/2$ and length $\theta_5$ with two series open stubs of characteristic impedance $Z_{oo5}$ and length $\theta_5$ at its two ends, as shown in Fig. 13(b) [21]. Each

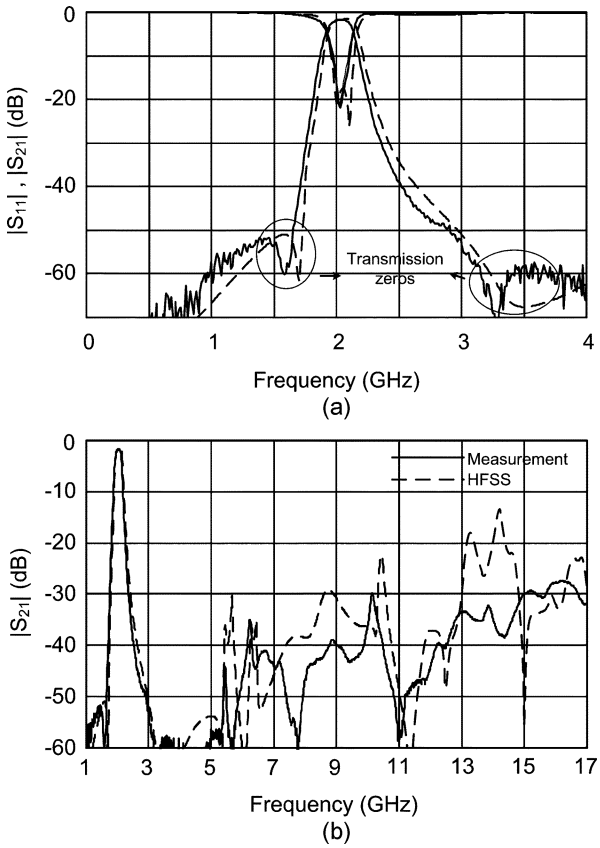


Fig. 14. Measured and simulated results for the proposed fourth-order microstrip bandpass filter in Fig. 10. (a) Narrow- and (b) wide-band frequency responses.

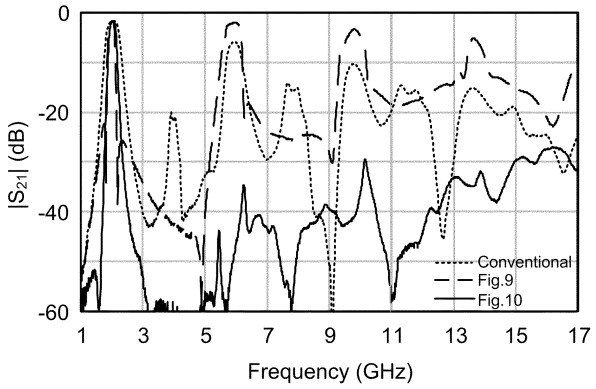


Fig. 15. Comparison of measured response for the proposed filter structure in Fig. 10 with that for the one in Fig. 9 [16] and that for the conventional parallel coupled-line filter.

open stub of characteristic impedance $Z_{oo5}$ and length $\theta_5$ in Fig. 13(b) is further split into two open stubs of characteristic impedances $Z_{s5} = (Z_{oe5} + Z_{oo5})/2$ and $-Z_{d5} = -(Z_{oe5} - Z_{oo5})/2$, as shown in Fig. 13(c). The transmission-line section of$(Z_{d5}, \theta_5)$ in Fig. 13(c) is then combined with the two series stubs of $(-Z_{d5}, \theta_5)$ to form the $J$-inverter $(J_{54})$, as shown in Fig. 13(d), where $J_{54} = |\sin\theta_5/Z_{d5}|$.

The fourth-order filter (Fig. 10) is designed with a center frequency of 2.07 GHz, 3-dB bandwidth of 10%, according to a fourth-order maximally flat response. The corresponding circuit parameters are obtained as follows: $Z_{oe1} = 74.6\ \Omega$, $Z_{oo1} = 38.3\,\Omega, Z_{oe3} = 73.1\,\Omega, Z_{oo3} = 38.6\,\Omega, Z_{oe5} = 52.2\,\Omega$, $Z_{oo5} = 47.9\ \Omega$, $\theta_1 = 64.5°$, $\theta_3 = 70°$, $\theta_5 = 81.8°$ at 2 GHz, and $L = 0.26$ nH. The geometrical parameters are obtained by fine tuning in HFSS and are given in Fig. 10.

The measured and simulated results are shown in Fig. 14. The measured center frequency is at 2.03 GHz. The minimum measured insertion loss is 1.6 dB at 2.07 GHz, and the 3-dB bandwidth is 10.8%. The spurious responses are suppressed up to $7.4f_o$, and the harmonic rejection is better than 30 dB from 2.35∼14.8 GHz. Here, the microstrip coupled-line of length $l_5$ in Fig. 11 has a higher order inherent transmission zero around 13.5 GHz such that the spurious response at $7f_o$ is also slightly suppressed. Two cross-coupled-induced transmission zeros are found at 1.59 and 3.28 GHz, as expected. Good agreement between measured and simulated results is observed, except for a slight frequency shift.

To demonstrate the behavior in suppressing the spurious harmonics, Fig. 15 compares the measured response of the proposed filter in Fig. 10 with that of the filter structure in Fig. 9 [16] and that of the conventional parallel coupled-line filter. Note that great improvement on the spurious rejection has been achieved with almost the same circuit area. The total length of the proposed filter is only $5\lambda/9$ long, which is more compact than that of the filter in [13].

## IV. Conclusions

In this paper, a class of novel microstrip coupled-line bandpass filters with shortened coupled sections to extend the rejection band has been proposed and carefully examined. By using the inherent transmission zeros associated with the shortened coupled sections to suppress the spurious responses, a filter with extended rejection band can be achieved. This technique has the advantage of compact circuit size without increasing the insertion loss. Two microstrip coupled-line bandpass filters based on the shortened coupled sections have been implemented. Specifically, the second- and fourth-order bandpass filters have been designed with the rejection band extended up to $4.6f_o$ and $7.4f_o$, respectively. In addition, two cross-coupled-induced transmission zeros at the upper and lower stopbands have been introduced such that the filter selectivity may be improved. The proposed bandpass filters feature compact size, low loss, and are useful for applications in the communication system designs when high selectivity and good stopband rejection are required.

## References

[1] B. Easter and K. A. Merza, "Parallel-coupled-line filters for inverted-microstrip and suspended-substrate MICs," in *11th Eur. Microw. Conf. Dig.*, 1981, pp. 164–167.

[2] C.-Y. Chang and T. Itoh, "A modified parallel-coupled filter structure that improves the upper stopband rejection and response symmetry," *IEEE Trans. Microw. Theory Tech.*, vol. 39, no. 2, pp. 310–314, Feb. 1991.

[3] I. J. Bahl, "Capacitively compensated high performance parallel coupled microstrip filters," in *IEEE MTT-S Int. Microw. Symp. Dig.*, 1989, pp. 679–682.

[4] A. Riddle, "High performance parallel coupled microstrip filters," in *IEEE MTT-S Int. Microw. Symp. Dig.*, 1988, pp. 427–430.

[5] J.-T. Kuo, W.-H. Hsu, and W.-T. Huang, "Parallel coupled microstrip filters with suppression of harmonic response," *IEEE Microw. Wireless Compon. Lett.*, vol. 12, no. 10, pp. 383–385, Oct. 2002.
[6] T. Lopetegi, M. A. G. Laso, J. Hernandez, M. Bacaicoa, D. Benito, M. J. Garde, M. Sorolla, and M. Guglielmi, "New microstrip 'wiggly-line' filters with spurious passband suppression," *IEEE Trans. Microw. Theory Tech.*, vol. 49, no. 9, pp. 1593–1598, Sep. 2003.
[7] J.-T. Kuo and M. Jiang, "Suppression of spurious response for microstrip bandpass filters via substrate suspension," in *Asia–Pacific Microw. Conf.*, 2002, pp. 498–500.
[8] J.-T. Kuo, M. Jiang, and H.-J. Chang, "Design of parallel-coupled microstrip filters with suppression of spurious resonances using substrate suspension," *IEEE Trans. Microw. Theory Tech.*, vol. 52, no. 1, pp. 83–89, Jan. 2004.
[9] M. d. C. Velazquez-Ahumada, J. Martel, and F. Medina, "Parallel coupled microstrip filters with ground-plane aperture for spurious band suppression and enhanced coupling," *IEEE Trans. Microw. Theory Tech.*, vol. 52, no. 3, pp. 1082–1086, Mar. 2004.
[10] J. Garcia-Garcia, F. Martin, F. Falcone, J. Bonache, I. Gil, T. Lopetegi, M. A. G. Laso, M. Sorolla, and R. Marques, "Spurious passband suppression in microstrip coupled line band pass filters by means of split ring resonators," *IEEE Microw. Wireless Compon. Lett.*, vol. 14, no. 9, pp. 416–418, Sep. 2004.
[11] J.-T. Kuo, S.-P. Chen, and M. Jiang, "Parallel-coupled microstrip filters with over-coupled end stages for suppression of spurious responses," *IEEE Microw. Wireless Compon. Lett.*, vol. 13, no. 10, pp. 440–442, Oct. 2003.
[12] S.-M. Wang, C.-H. Chi, M.-Y. Hsieh, and C.-Y. Chang, "Miniaturized spurious passband suppression microstrip filter using meandered parallel coupled lines," *IEEE Trans. Microw. Theory Tech.*, vol. 53, no. 2, pp. 747–753, Feb. 2005.
[13] J.-T. Kuo and E. Shih, "Microstrip stepped impedance resonator bandpass filter with an extended optimal rejection bandwidth," *IEEE Trans. Microw. Theory Tech.*, vol. 51, no. 5, pp. 1554–1559, May 2003.
[14] Y.-S. Lin and C. H. Chen, "Novel balanced microstrip coupled-line bandpass filters," in *URSI Int. Electromagn. Theory Symp.*, 2004, pp. 567–569.
[15] C.-H. Wang, Y.-S. Lin, and C. H. Chen, "Novel inductance-incorporated microstrip coupled-line bandpass filters with two attenuation poles," in *IEEE MTT-S Int. Microw. Symp. Dig.*, 2004, pp. 1979–1982.
[16] Y.-S. Lin, C.-H. Wang, C.-H. Wu, and C. H. Chen, "Novel compact parallel-coupled microstrip bandpass filters with lumped-element $K$-inverters," *IEEE Trans. Microw. Theory Tech.*, vol. 53, no. 7, pp. 2324–2328, Jul. 2005.
[17] G. L. Mattaei, L. Young, and E. M. T. Jones, *Microwave Filters, Impedance-Matching Networks, and Coupling Structures*. Norwood, MA: Artech House, 1980.
[18] D. M. Pozar, *Microwave Engineering*, 2nd ed. New York: Wiley, 1998.
[19] G. L. Mattaei, "Direct-coupled, bandpass filters with $\lambda_o/4$ resonators," in *IRE Nat. Conv. Rec.*, 1958, pp. 98–111.
[20] A. E. Ruehli, "Inductance calculations in a complex integrated circuit environment," *IBM J. Res. Develop.*, vol. 16, pp. 470–481, Sep. 1972.
[21] G. L. Matthaei, "Design of wide-band (and narrow-band) bandpass microwave filters on the insertion loss basis," *IRE Trans. Microw. Theory Tech.*, vol. MTT-8, no. 11, pp. 580–593, Nov. 1960.

**Chao-Huang Wu** was born in Taoyuan, Taiwan, R.O.C., in 1980. He received the B.S. degree in electrical engineering from the National Sun Yet-Sen University, Kaohsiung, Taiwan, R.O.C., in 2002, and is currently working toward the Ph.D. degree in communication engineering at the National Taiwan University, Taipei, Taiwan, R.O.C.

His research interests include the design and analysis of microwave filter circuits.

**Yo-Shen Lin** (M'04) was born in Taipei, Taiwan, R.O.C., in 1973. He received the B.S. and M.S.E.E. degrees in electrical engineering and Ph.D. degree in communication engineering from National Taiwan University, Taipei, Taiwan, R.O.C., in 1996, 1998, and 2003, respectively.

From 1998 to 2001, he was an RF Engineer with Acer Communication and Multimedia Inc., Taipei, Taiwan, R.O.C., where he designed global system for mobile communication (GSM) mobile phones. From 2001 to 2003, he was with Chi-Mei Communication System Inc., Taipei, Taiwan, R.O.C. where he was involved with the design of low-temperature co-fired ceramic (LTCC) RF transceiver modules for global system for mobile communications (GSM) mobile applications. In August 2003, he joined the Graduate Institute of Communication Engineering, National Taiwan University, as a Post-Doctoral Research Fellow, and became an Assistant Professor in August 2004. Since August 2005, he has been with the Department of Electrical Engineering, National Central University, Chungli, Taiwan, R.O.C., where he is currently an Assistant Professor. His research interests include the design and analysis of miniature planar microwave circuits and RF transceiver module for wireless communication systems.

Dr. Lin was the recipient of the Best Paper Award of the 2001 Asia–Pacific Microwave Conference (APMC), Taipei, Taiwan, R.O.C., and the 2005 Young Scientist Award presented at the URSI General Assembly, New Delhi, India.

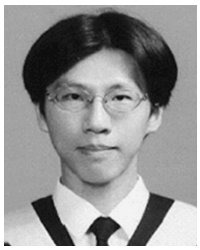

**Chi-Hsueh Wang** was born in Kaohsiung, Taiwan, R.O.C., in 1976. He received the B.S. degree in electrical engineering from National Cheng Kung University, Tainan, Taiwan, R.O.C., in 1997, and the Ph.D. degree from National Taiwan University, Taipei, Taiwan, R.O.C. in 2003.

He is currently a Post-Doctoral Research Fellow with the Graduate Institute of Communication Engineering, National Taiwan University. His research interests include the design and analysis of microwave and millimeter-wave circuits and computational electromagnetics.

**Chun Hsiung Chen** (SM'88–F'96) was born in Taipei, Taiwan, R.O.C., on March 7, 1937. He received the B.S.E.E. and Ph.D. degrees in electrical engineering from National Taiwan University, Taipei, Taiwan, R.O.C., in 1960 and 1972, respectively, and the M.S.E.E. degree from National Chiao Tung University, Hsinchu, Taiwan, R.O.C., in 1962.

In 1963, he joined the Faculty of the Department of Electrical Engineering, National Taiwan University, where he is currently a Professor. From August 1982 to July 1985, he was Chairman of the Department of Electrical Engineering, National Taiwan University. From August 1992 to July 1996, he was the Director of the University Computer Center, National Taiwan University. In 1974, he was a Visiting Scholar with the Department of Electrical Engineering and Computer Sciences, University of California at Berkeley. From August 1986 to July 1987, he was a Visiting Professor with the Department of Electrical Engineering, University of Houston, TX. In 1989, 1990, and 1994, he visited the Microwave Department, Technical University of Munich, Munich, Germany, the Laboratoire d'Optique Electromagnetique, Faculte des Sciences et Techniques de Saint-Jerome, Universite d'Aix-Marseille III, Marseille, France, and the Department of Electrical Engineering, Michigan State University, East Lansing, respectively. His areas of interest include microwave circuit analysis and computational electromagnetics.